IEEE Access
Multidisciplinary ⋮ Rapid Review ⋮ Open Access Journal

Received 19 October 2022, accepted 26 November 2022, date of publication 2 December 2022,
date of current version 12 December 2022.

Digital Object Identifier 10.1109/ACCESS.2022.3226670

RESEARCH ARTICLE

An Adaptive Neuro-Fuzzy Control Strategy for Improved Power Quality in Multi-Microgrid Clusters

S. N. V. BRAMARESWARA RAO[1], Y. V. PAVAN KUMAR[2], (Member, IEEE), MOHAMMAD AMIR[3], (Member, IEEE), AND FURKAN AHMAD[4], (Member, IEEE)

[1]Department of Electrical and Electronics Engineering, Sir C. R. Reddy College of Engineering, Eluru, Andhra Pradesh 534007, India
[2]School of Electronics Engineering, VIT-AP University, Amaravati, Andhra Pradesh 522237, India
[3]Department of Electrical Engineering, Faculty of Engineering and Technology, Jamia Millia Islamia (A Central University), Delhi 243601, India
[4]Division of Sustainable Development, College of Science and Engineering, Hamad Bin Khalifa University, Qatar Foundation, Doha, Qatar

Corresponding authors: Y. V. Pavan Kumar (pavankumar.yv@vitap.ac.in) and Furkan Ahmad (fuahmad@hbku.edu.qa)

This work was supported by the Qatar National Library.

ABSTRACT Microgrids are being evolved as a potential alternative to reduce unrelenting dependency on central utility grids. Moreover, integrated multi-microgrid based clusters are forming in closed vicinities to enhance the benefits of microgrids. However, the power quality problem is one of the key issues to be solved in such systems, which is mainly caused by the rising penetration of nonlinear loads and interfacing of power electronic converters. To address this issue, this paper proposes a new control technique, named ''adaptive neuro-fuzzy control strategy''. This controls the inverter of each microgrid in the cluster as well as the voltage source converter-based distribution static compensator located at the point of common coupling between the cluster and the utility grid. This proposed control strategy uses the advantages of both fuzzy logic and artificial neural networks, thereby effectively controlling the system. The proposed technique is modelled in MATLAB/Simulink software 2021a. For the analysis, various power quality indices such as voltage sag/swell, voltage unbalance, frequency deviations, power characteristics, total harmonic distortion, and neutral current compensation are measured. These indices of the proposed controller are compared with conventional PI and fuzzy logic-based controllers in view of various key IEEE/IEC standard tolerances. From these results, the proposed controller has proved its superiority.

INDEX TERMS Power quality, multi-microgrids, adaptive neuro-fuzzy control strategy, distribution static compensator, proportional integral, fuzzy control.

NOMENCLATURE

Parameters

θ	Phase angle.
P_G	Power generation.
e	Error.
Δe	Change in error.
$V_{M.D}$	Maximum deviation in voltage.
$\tilde{\omega}_\alpha$	Normalized firing strength.
$\bar{y}_i$	Forecasted value.
ω	Fundamental angular frequency.
$I_{\alpha L}^{MG,i}$, $I_{\beta L}^{MG,i}$	Stationary frame variables.
K_{pd}, K_{id}	PI controller gain.
V_{DC}^{*}	Reference DC value.

Abbreviations

ANFCS	Adaptive neuro-fuzzy control strategy.
DNN	Deep neural network.
D-STATCOM	Distributed static compensator.
FLC	Fuzzy logic controller.
LAC	Local agent controller.
MAE	Mean average error.
MMGs	Multi-microgrids.
MFs	Membership functions.

The associate editor coordinating the review of this manuscript and approving it for publication was Arup Kumar Goswami.

PCC	Point of common coupling.
PSO	Particle swarm optimization.
SMC	Sliding mode control.
SPV	Solar photovoltaic.
THD	Total harmonic distortion.
UPQC	Unified power quality controller.

I. INTRODUCTION

The need to provide resources and technology to address the energy needs of rural areas and/or places, where power is unavailable are the typical driving force behind microgrid research. However, due to the present globalization era, people from rural and remote areas are moving to cities, creating a burden on the electricity grid [1], [2]. As a result, urban areas are now at the center of microgrid design. This improves the quality and dependability of the consumer supply of electric power while offsetting the worldwide depletion of conventional fossil fuel-based electric grid energy [3]. Additionally, integrating neighboring microgrids in a community makes it easier for them to share power rather than relying entirely on the utility grid. Similarly, power electronic-based inverters play a crucial role today with the significant penetration of DG sources in the distribution grid. These power electronic systems' properties are nonlinear, resulting in a distorted waveform. This demonstrates a negative impact on the quality of the power the distribution firm provides to clients and results in a high cost of energy [4]. The challenges mentioned above motivate the power system researchers to scale up the design of microgrid clusters from the level of a single building to that of an urban community. Different power quality improvement devices, such as the ''Dynamic Voltage Restorer,'' ''Automatic Voltage Regulator,'' ''Distributed Static Compensator (D-STATCOM),'' and ''Unified Power Quality Controller (UPQC),'' have been developed by researchers to enhance the power quality (PQ) indices such voltage fluctuations, frequency deviations, harmonic distortion of microgrids. The topologies of inverters controlled by contemporary modulation and alternative conversion techniques to replace power electronic inverters and accounting for uncertainty when designing storage units for energy management are the three main areas of research being done to address the aforementioned PQ issues. The most recent research for enhancing the power quality in distribution systems is summarized as follows.

For the grid integration of PV systems, a new cascaded multilevel inverter is presented along with a maximum power point tracking method based on an artificial intelligence controller. The suggested inverter can reduce total harmonic distortion (THD) at the output side by raising the output voltage level, improving the system's power quality [5]. Similarly, in [6] wind energy-based microgrid with a unified power quality conditioner is proposed, and appropriate control methods are designed for the UPQC's series and shunt converters. Higher power quality improvement is made under various load scenarios using a PSO optimization technique. However, [7] proposed a proportional-integral-derivative controller with an adaptively switched filter compensator to enhance the MMG's overall dynamic performance. Since operating circumstances may change while an MMGs is operating, the grasshopper optimization algorithm is used to apply the best tuning to the PID's controller gains. It is also suggested to use D-STATCOM, one of the most common D-FACTS, with an optimally tuned PID controller. Later an advanced three-phase four-wire interlinking microgrid system with a better harmonics reduction feature is presented in [8] research. This research proposes a sophisticated control system with improved harmonics reduction functionality for use in microgrid applications. Compared to traditional notch-filter-based techniques, the suggested control system has a greater harmonics reduction feature and better dynamic response. Moreover, the authors in [9] suggest an efficient control approach for UPQC based on the dq0 detection method to address the drawbacks of traditional compensation control strategies and improve the compensating impact of UPQC. This work also makes improvements to the space vector pulse width modulation technique. To estimate reference current for improving power quality, modified synchronous reference frame control of the PV inverter has been proposed in [10]. In this work, a fuzzy logic controller (FLC) based on interval type-2 has been presented to manage the DC link voltage of the inverter. Grid-connected solar photovoltaic (SPV) system performance is examined utilizing suggested IT-2 FLC and contrasted with traditional PI and type-1 FLC. To reduce current harmonics, the study in [11] assesses the effectiveness of the modified synchronous reference frame extraction technique using an FLC-based current control pulse width modulation inverter of a three-phase three-wire shunt active filter. Due to the suggested FLC's reduced use of membership functions and rules, calculation time and memory usage are significantly decreased. In [12], shunt hybrid filters are used to concentrate greater attention on PQ improvement in the multi-microgrid (MMGs) system, which is a component of SG (SHF). An enhanced and cutting-edge regulating method, adaptive fuzzy-neural network control is used to explore the working of SHF to provide an effective SG subjected to various loads and supply voltage scenarios.

Moreover, [13] has used deep neural networks (DNN) and maximum power point tracking to design a novel model for the efficient working of photovoltaic and wind-based based power generation systems. A cutting-edge DNN controller was designed to integrate a hybrid P.V./wind energy system into a microgrid while enhancing power quality and lowering THDs. Based on two clever decoupled controllers, a control method for a battery energy storage system is developed [14]. The goal is to restore system voltage and frequency while taking into account a variety of disturbances to avoid a decline in power quality. The suggested controller is based on a hybrid neural network with differential evolution optimization. Later in [15], to make grid-integrated power

systems more intelligent, a suggested $I\cos\varphi$ control algorithm for power sharing and power quality enhancement in smart microgrid systems is based on artificial intelligence. The presented controller takes into account several variables brought on by changes in load, the microgrid battery's state of charge, and power tariffs based on the availability of electricity in microgrids. Authors in [16] have shown a fused control scheme for the VSC of DSTATCOM. It is based on the second-order super twisting algorithm and sliding mode control (SMC), and it effectively eliminates the effects of voltage sag/swell and compensates for active and reactive power in distribution systems. STA is combined with normal SMC to overcome the chattering effect, which is a weakness of SMC alone, while maintaining its other benefits, such as robustness, quicker response times, and load variation insensitivity. To combat the shoot-through effect and lessen supply current distortions, a three-phase four-wire multilevel inverter-based active power filter is presented in [17]. Utilizing a hysteresis current controller and an adaline-based LMS algorithm, the voltage source inverter is controlled. In [18], the effective operation of a fuel cell stack feeding a nonlinear load connected to the grid is described. Using a shunt active power filter (SAPF) connected in parallel at the point of common coupling optimizes the operation (PCC). Optimizing the SAPF settings using the gravitational search algorithm and improved particle swarm optimization maintains the power quality.

According to the above-discussed research literature, the following research gaps are identified.

- Concerning PQ improvements, most of the conducted studies are limited to single microgrids modeled with solar/wind energy sources.
- Most of the research literature has focused on improving either voltage swell/sag or THD.

The inverter in a microgrid cluster with an improved power quality characteristic is controlled by the new control technique proposed in this paper, which is based on an adaptive Neuro-Fuzzy Control Strategy. The motivation behind the proposed methodology is adopted from [1]. ANFCS can combine the advantages of fuzzy logic and neural networks into a single framework because it incorporates both of these concepts. The following are the key contributions of this research work.

- A multi-microgrid cluster system is proposed with the integration of neighborhood microgrids to effectively utilize locally available renewable energy sources in all microgrids.
- An adaptive neuro-fuzzy control strategy is proposed to enhance the power quality for the inverter of the ith microgrids.
- Further, this manuscript has modeled a voltage source converter-based DSTATCOM for neutral current compensation in a microgrid cluster system.

The rest of the paper is structured as follows. The proposed multi-microgrid cluster system along with its constituents is presented in Section II. The analysis of the proposed controller is demonstrated in Section III, and Section IV demonstrates the effectiveness of the suggested controller through simulation findings under various testing scenarios, followed by the paper's conclusion in Section V.

II. DESCRIPTION AND MODELING OF THE PROPOSED SYSTEM AND ITS CONSTITUENTS

The structure of the proposed microgrid cluster is shown in Fig. 1. The proposed system is formed by integrating the different green buildings with different energy and load profiles. Each green building is considered a single microgrid associated with its locally available renewable energy sources. This work has adopted the mathematical modeling of renewable energy sources and the conventional inverter from [19] and [20]. Each microgrid is designed with a controller called the local agent controller of the said microgrid. These local agent controllers of all the microgrids communicate with the central monitoring control unit for making energy transactions with the grid utility, which is connected at the point of common coupling of the cluster.

A. MODELING OF LOCAL AGENT CONTROLLER

Based on the multi-agent theory, the local agent controller (LAC) model implemented in MATLAB/Simulink, as shown in Fig. 2, functions as an agent. [21], [22]. It is a DC (or A.C.) to DC converter combined with a switch (toggle). The LAC controls the associated energy source or loads connectivity to the microgrid using an input control signal from the central energy management system. Figure 3 shows the procedure for implementing agent control logic in the i^{th} microgrid of the proposed multi-microgrid cluster in all the microgrids using MATLAB/Simulink software. The same sequences of operations are followed for all other microgrids, thereby managing the power flow at the community itself. This collectively decreases the burden on the utility grid.

B. MODELING OF DC BUS

Through the DC bus, all resources are connected in parallel. As part of a centralized DC bus design, the output of energy resources is initially provided to the local controller and then to the DC bus. Figure 4 illustrates the MATLAB/Simulink model of the DC bus. From this source, DC power is provided to the remaining components of the system. The DC bus also supplies an inverter system at the next level.

C. MODELING OF CENTRAL ENERGY MANAGEMENT SYSTEM (CEMS)

The CEMS theory essentially operates under the following three conditions:

- The power generation (P_G) is equal to load power (P_D) when there is sufficient power available.
- The power generation (P_G) is greater than load power (P_D) under excess power conditions.

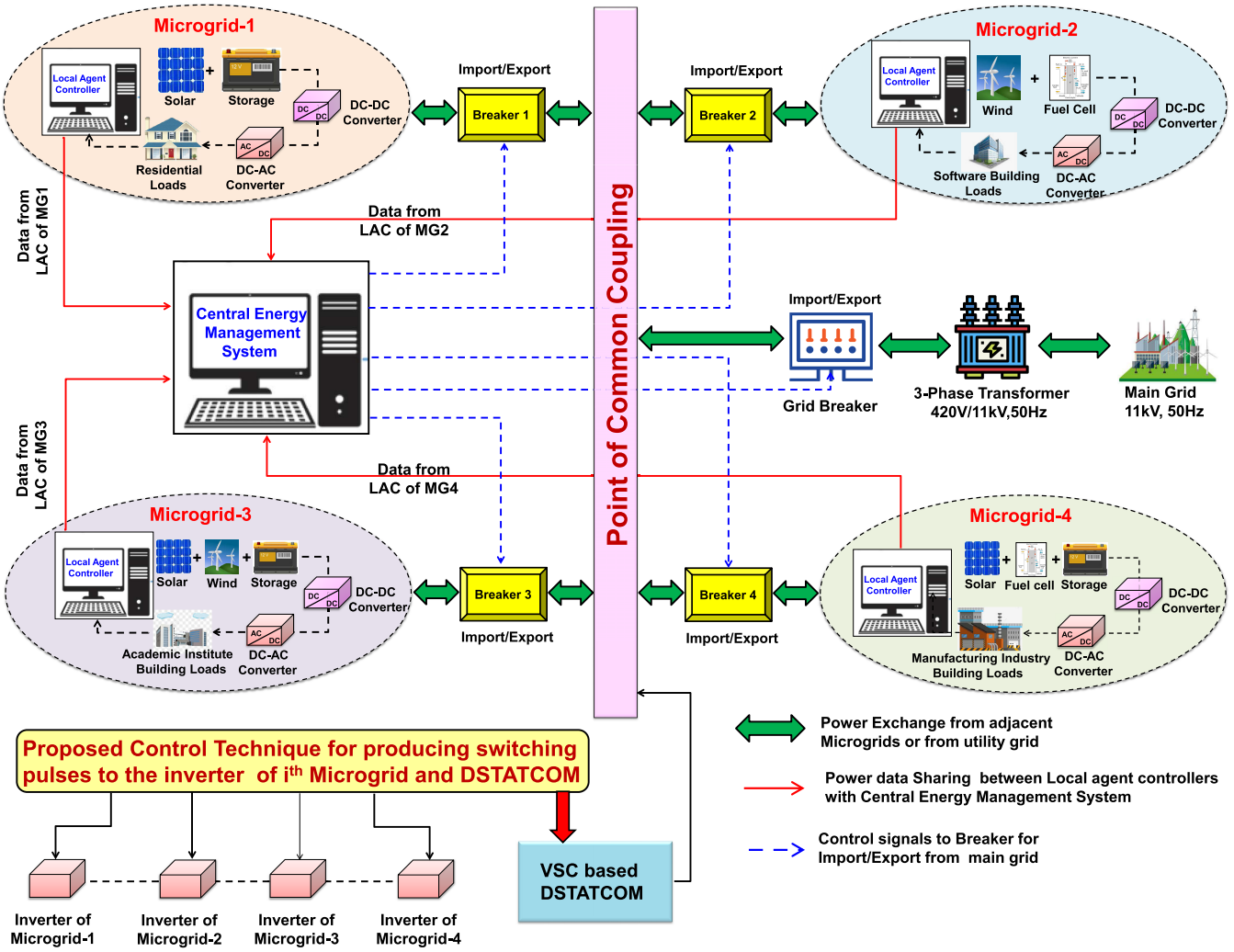

FIGURE 1. Structure of proposed multi-microgrid cluster.

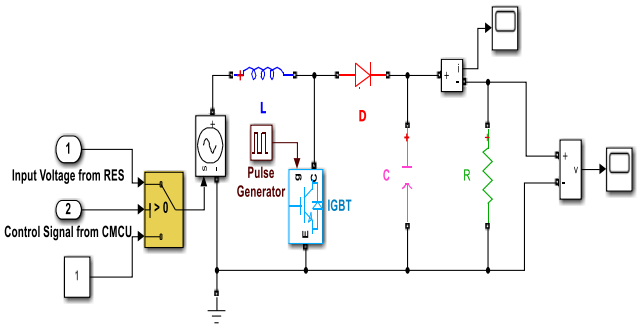

FIGURE 2. Modeling of local agent controller in MATLAB/Simulink.

- The power generation (P_G) is less than load power (P_D) under deficit power conditions.

The aggregate of all energy resource outputs is known as total power generated P_G ($P_{DC,Bus}$). The aggregate demand for all sorts of loads is known as total demand P_D (Primary Load (L_P) and Secondary Load (L_S)). Wind and solar PV are always ON because they have no fuel input costs. When P_G and P_D are equal, there is enough power.

The CEMS unit won't disrupt the system, allowing it to continue operating as normal until the advent of any problem; it remains in the previous state. Still, P_G stands for excess power generation, which is more than P_D and is employed to produce hydrogen for charging the batteries or the fuel cells electrolyzer.

If the CEMS still detects too much power, it directs grid exchange to export surplus energy to the utility grid. P_G is smaller than P_D, which denotes a power deficit; in this situation, the fuel cell unit is turned ON, and the battery and fuel cell charging is OFF. Additionally, the batteries are run according to demand, and even more, it is in deficit; utility companies supply the balance of the power. Figure 5 shows the implementation of the central energy management system in the MATLAB/Simulink environment.

D. MODELING OF D-STATCOM

Six insulated gate bipolar transistors (IGBT) are used in the three-phase voltage source converter (VSC), which also serves as the D-STATCOM and antiparallel diodes are

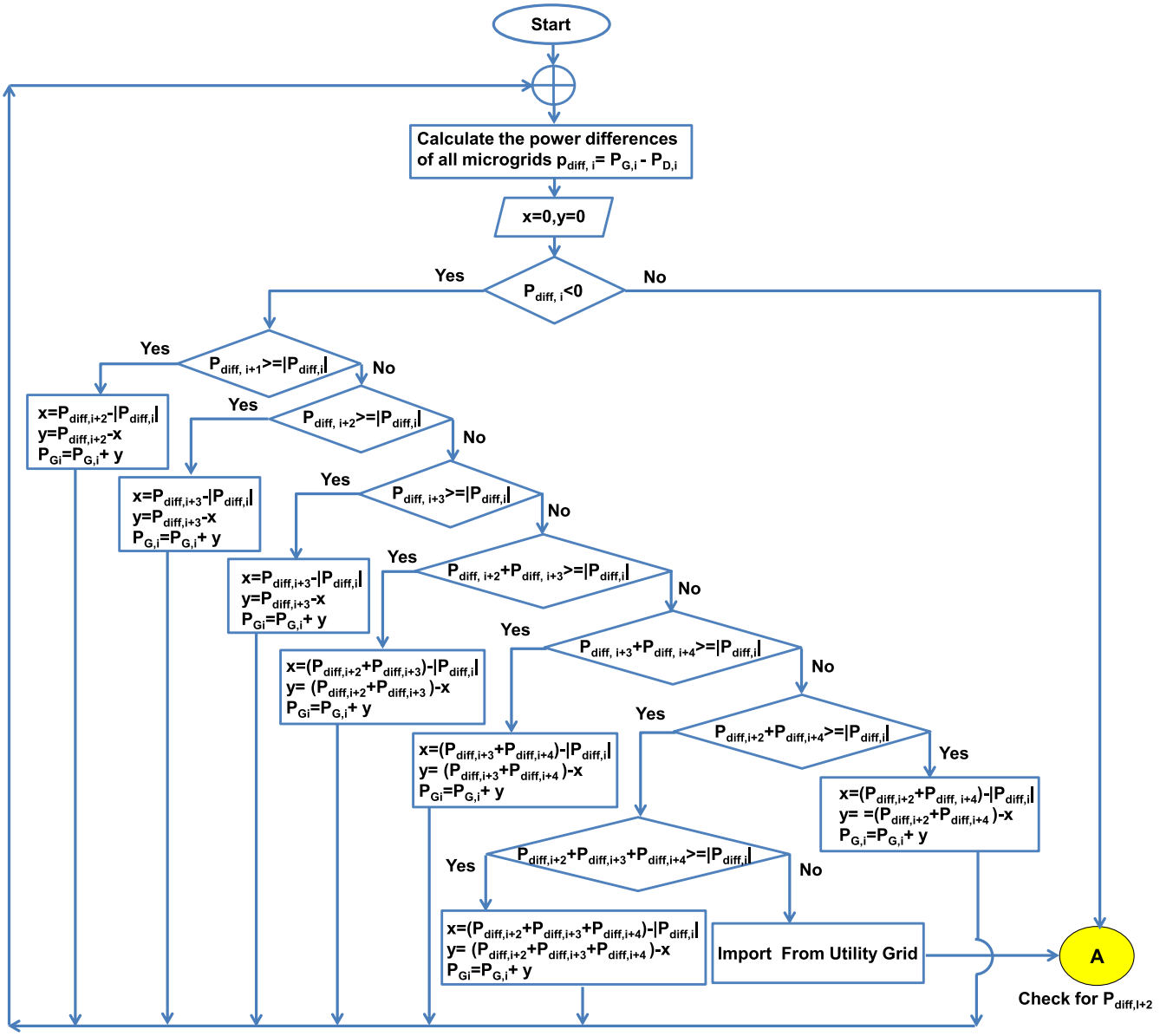

FIGURE 3. Flowchart for implementing local agent controller of microgrid-1 of the cluster.

connected to each IGBT. Figure 6 shows the schematic of the proposed D-STATCOM that is to be connected at PCC.

The capacitor on the DC side of the voltage source converter is utilized to keep the voltage constant during the switching operation of the IGBT switches. Reactive power adjustment is not performed using the DC capacitor. Between D-STATCOM and the load, the storage capacitor C_{DC} does not exchange any active power. Breaker is used to track the D-STATCOM's performance before and after compensating.

III. PROPOSED ANFCS-BASED CONTROL STRATEGY

A. DESIGN OF ANFCS CONTROLLER

An adaptive neuro-fuzzy control strategy was modeled using MATLAB's fuzzy toolbox. A fuzzy inference system, membership functions (MFs) for input and output, rules viewer, and output surface are some of its characteristics. The range and number of MFs are adjustable and are determined by the user. The Sugeno model, which ANFCS employs, provides the ability to change the MFs and their flexible range. The hybrid optimization methodology is a method for calculating various frameworks using the total deviation and the square of the actual and expected output. Time efficiency and ease of use are the two key benefits of employing ANFCS. Because ANFCS does not require human expert knowledge, it uses the least time and is easier to use when choosing parameters and optimizing MFs, and promotes sustainability. The ANFCS framework functions in two distinctive stages: the neural-network stage, when it organizes data and finds

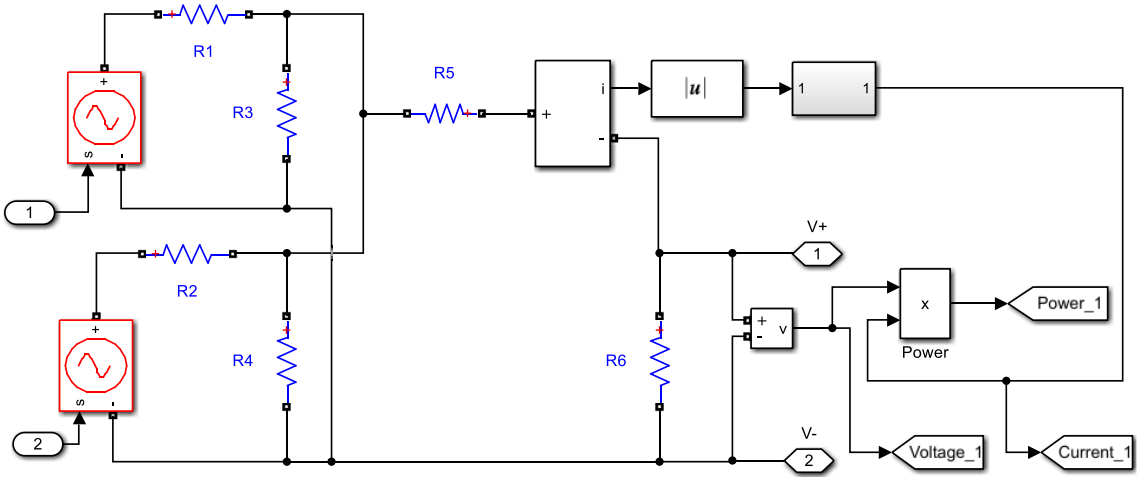

FIGURE 4. DC bus modeled in MATLAB/Simulink.

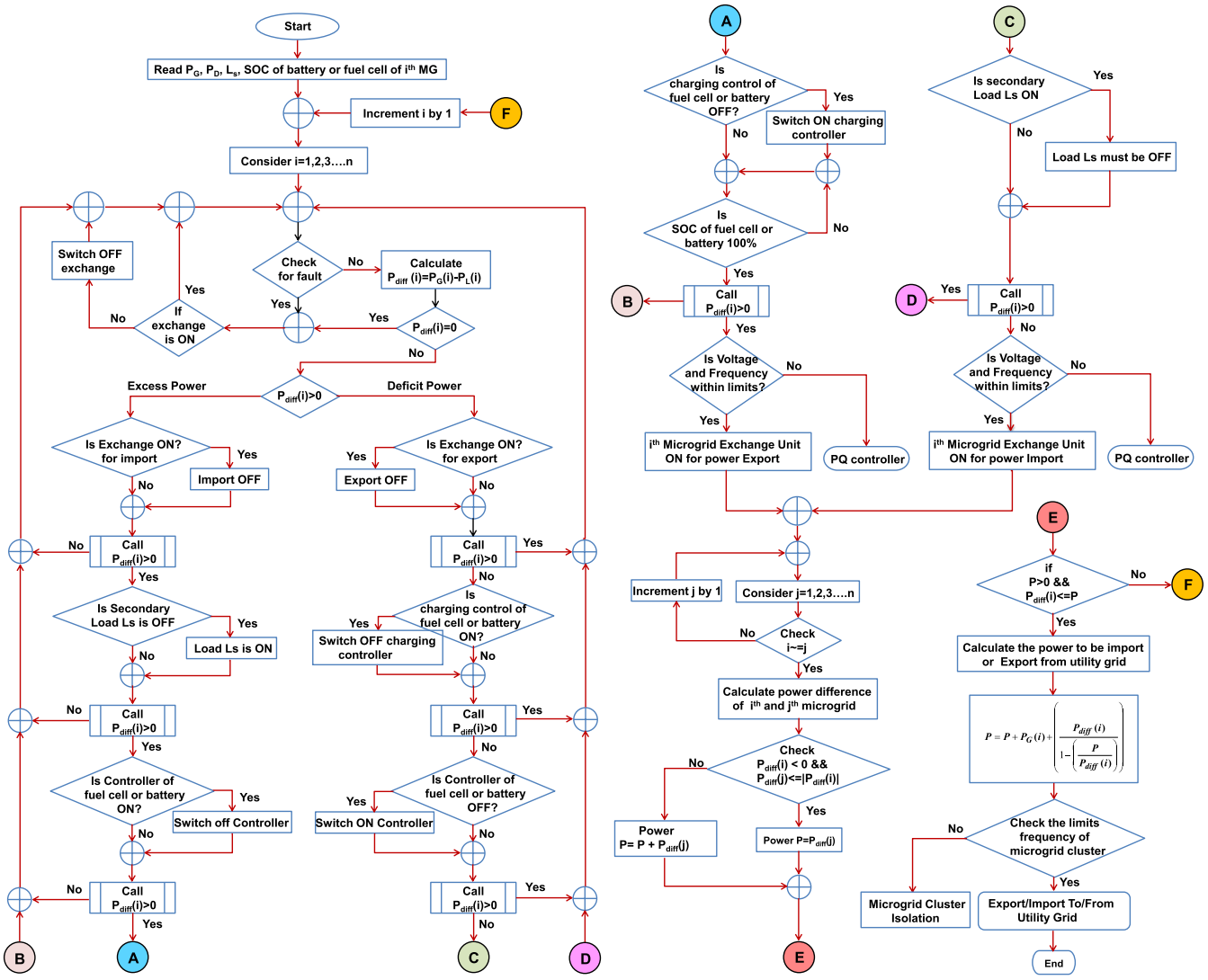

FIGURE 5. Flow chart for implementing central energy management system (CEMS).

patterns. The other step promotes a flexible tuning of participation capacities that encourages a fuzzy master framework. A fuzzy inference system (FIS) is generated using input and output data pairs. At the same time, the least-squares

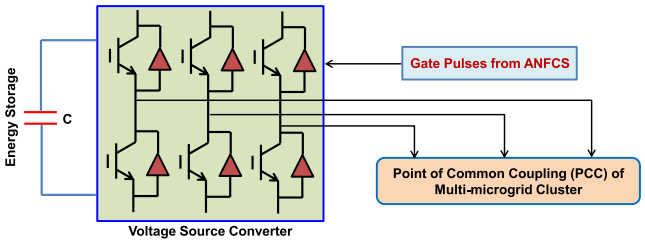

FIGURE 6. Schematic view of D-STATCOM.

approach, a backpropagation algorithm, or a mix of both is used to tune the membership functions. The output parameters for the ANFCS are known as nonlinear parameters, whereas the input parameters are known as linear parameters. The knowledge base for this system is composed of two fuzzy input-based if-then rules, which are given by the following rules.

Rule 1: if 'e' is A_1 and 'Δe' is B_1 then $f_1 = m_1e+n_1\Delta e+p_1$

Rule 2: if 'e' is A_2 and 'Δe' is B_2 then $f_2 = m_2e+n_2\Delta e+p_2$

Where A_1, B_1, A_2, and B_2 are fuzzy set parameters of each linguistic input; f_1 and f_2 are the output functions; m_1, m_2, n_1, n_2, p_1, and p_2 are linear parameters of the i^{th} rule. The ANFCS structure consists of five layers with two inputs and single output as shown in Fig. 7 [24].

- Layer 1: The purpose of this layer is to fuzzify nonlinear input using linguistic factors like small, medium, and large. The membership functions specified in these linguistic parameters are used to determine this layer's output. The parameters in this layer are referred to as nonlinear parameters, and the node is adaptive. Each node's mathematical expression is given in Eq. (1) [25],

$$\left.\begin{aligned}\lambda_{1,\alpha} &= \psi_{A\alpha}(e)\\ \lambda_{1,\alpha} &= \psi_{B\alpha}(\Delta e)\end{aligned}\right\} \; where, \quad \alpha = 1, 2, 3 \ldots . \beta \quad (1)$$

where α represents neuron number, 'e' and 'Δe' are error and change in error, which are used as inputs for node 1, $\psi_{A1}(e)$ and $\psi_{B1}(\Delta e)$ are the membership functions. A generalized bell-shaped membership function (gbellmf) is assigned for each node and is expressed in Eq. (2).

$$\psi(x; m, n, p) = \frac{1}{1 + \left|\frac{x-p}{m}\right|^{2n}} \quad (2)$$

It mainly manages non-fuzzy sets and depends on three parameters: m, n, and p.

- Layer 2: The output of this layer is derived from the multiplication of all incoming signals at this node, designated as P. Eq. (3) represents the node function for this layer [25],

$$\lambda_{2,\alpha} = \psi_{A_\alpha}(e) * \psi_{B\alpha}(\Delta e); \quad \text{where, } \alpha = 1, 2 \quad (3)$$

- Layer 3: The nodes shown in this layer are responsible for performing the normalization process. These nodes are fixed and shown as circles with the letter N in them.

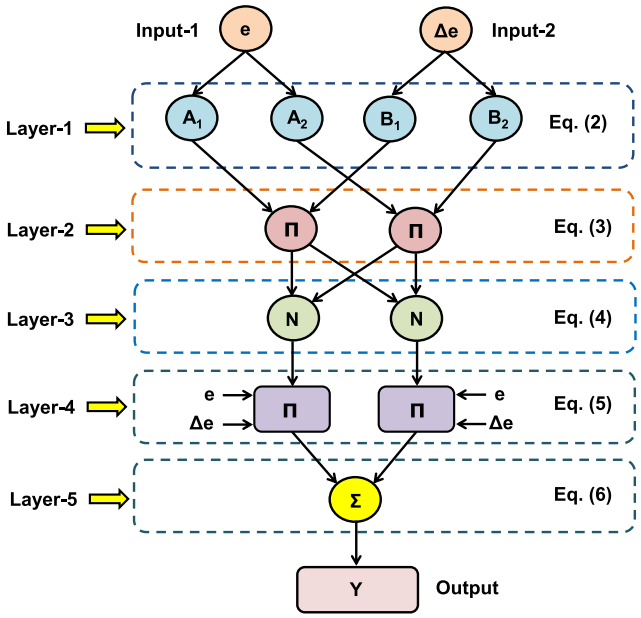

FIGURE 7. Typical architecture of ANFCS controller.

The output of this layer node is determined by dividing the ratio of the ring strength of each rule by the total ring strength of all the rules. The node function of layer 3 is given in Eq. (4) [25],

$$\lambda_{3,\alpha} = \tilde{\omega}_\alpha = \frac{\omega_\alpha}{\omega_1 + \omega_2}; \quad \text{where, } \alpha = 1, 2 \ldots \quad (4)$$

- Layer 4: This layer's node is considered an adaptive node. The node's function is expressed as Eq. (5) [25].

$$\lambda_{4,\alpha} = \tilde{\omega}_\alpha f_\alpha = \omega_\alpha(m_\alpha e + n_\alpha \Delta e + p_\alpha); \quad \alpha = 1, 2.. \quad (5)$$

where the normalized firing strength is shown by $\tilde{\omega}_\alpha$. ANFCS's training procedure modifies the linear parameters m_α, n_α, and p_α in Equation (5).

- Layer 5: A single fixed node with the letter S is present in the final layer, and it sums up all the input signals to get the following final output total given in Eq. (6) [25],

$$\lambda_{5,\alpha} = \frac{\sum_\alpha \tilde{\omega}_\alpha f_\alpha}{\sum_\alpha \tilde{\omega}_\alpha}; \quad \text{where } \alpha = 1, 2.. \quad (6)$$

B. TRAINING OF ANFCS CONTROLLER

At first, the PI controller is used to develop inverter control strategies; later, the PI controller is combined with the proposed ANFCS controller. The two inputs, i.e., 'e' and 'Δe', are considered to train the proposed controller, and the training process is clearly explained in Fig. 8.

With the MATLAB toolbox, the user can upload the input data, training data, and saved FIS file and open the final FIS file. The first step in using the toolbox is to collect the training data set. As this data will be used as an input value for the

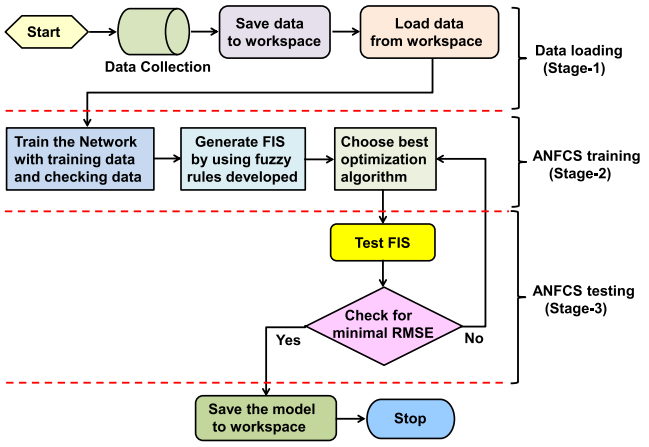

FIGURE 8. Flowchart representing the training process of the ANFCS.

TABLE 1. Parameters used for training the ANFCS controller.

S. No	Parameter	Value
1	Inputs	2
2	Output	1
3	Membership functions	49
4	Total Samples collected	200
5	Samples used for Training	160 (80%)
6	Samples used for Testing	40 (20%)
7	Total epochs	40
8	Type of membership function	gbellmf
9	Optimization algorithm	Hybrid

toolbox, it should be organized in a matrix format. All input columns of the matrix are referred to as input columns, while the final column refers to the output column. Depending on the system's needs, the matrix may have several columns. To train the proposed controller, 200 samples are considered. The parameters considered for training the proposed controller are shown in Table 1. A measure of the inaccuracy of the training can be obtained by calculating the root mean square error (RMSE) and the mean average error (MAE) using Eq. (7)-(8).

$$RMSE = \sqrt{\frac{1}{P}\left(\sum_{i}^{P}(y_i - \bar{y}_i)^2\right)} \tag{7}$$

$$MAE = \frac{1}{P}\left(\sum_{i}^{P}(y_i - \bar{y}_i)^2\right) \tag{8}$$

where P is the total forecasting value, y_i is the reference value, and $\bar{y}_i$ is the forecasted value. Figure 9 shows how effectively the controller is trained in the ith microgrid.

The controller developed by considering two inputs, i.e., 'e' and 'Δe', is measured using Eq. (9) and Eq. (10).

$$e = V_{dc}^{*} - V_{dc} \tag{9}$$

$$\Delta e = \frac{V_{dc}^{*} - V_{dc}}{V_{dc}^{*}} \tag{10}$$

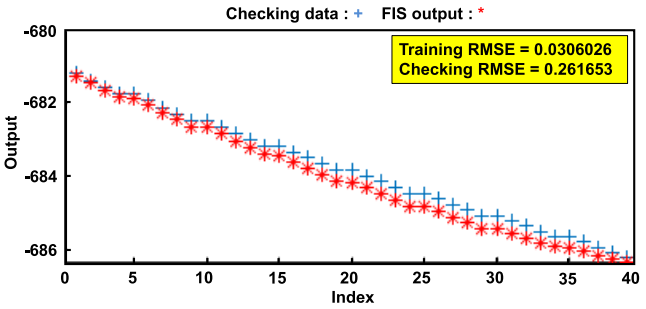

FIGURE 9. Accuracy of the data used for training the ANFCS controller.

where V_{dc}^{*}- reference DC value and V_{dc} is the actual DC value obtained from the ith microgrid. In the proposed microgrid cluster, we have designed a DC bus that produces a constant DC voltage at its output irrespective of the input renewable energy sources connected in each microgrid of the cluster.

C. GENERATION OF GATE PULSES

This study uses a novel control method to produce the reference signals. In the control process, low pass filters (LPFs) are utilized to reduce the harmonics of the input signals, even though these voltages are required to calculate the transformation angle. In this approach, harmonic interference from the source voltage is less likely to occur. Figure 10 depicts the proposed control circuit based on an ANFCS controller for generating switching pulses for the inverter of the ith microgrid.

The load currents of ith microgrid, $I_{aL}^{MG,i}$, $I_{bL}^{MG,i}$ and $I_{cL}^{MG,i}$ are transformed into stationary frame variables, i.e., $I_{\alpha L}^{MG,i}$ and $I_{\beta L}^{MG,i}$ using Eq. (11).

$$\begin{bmatrix} I_{L\alpha}^{MG,i} \\ I_{L\beta}^{MG,i} \end{bmatrix} = \begin{bmatrix} 1 & -1/2 & 1/2 \\ 0 & \sqrt{3}/2 & -\sqrt{3}/2 \end{bmatrix} \begin{bmatrix} I_{aL}^{MG,i} \\ I_{bL}^{MG,i} \\ I_{cL}^{MG,i} \end{bmatrix} \tag{11}$$

After that, for the transformation of the stationary frame (α-β) to the rotating frame (d-q), a unit vector generation circuit is used to produce proper sine and cosine signals to have synchronized with the voltage (utility).

$$\begin{bmatrix} I_{Ld}^{MG,i} \\ I_{Lq}^{MG,i} \end{bmatrix} = \begin{bmatrix} Sin\theta & -Cos\theta \\ Cos\theta & Sin\theta \end{bmatrix} \begin{bmatrix} I_{L\alpha}^{MG,i} \\ I_{L\beta}^{MG,i} \end{bmatrix} \tag{12}$$

where 'θ' represents the phase angle corresponding to the voltage of the ith microgrid. The amplitude of the unit sine vector is one under a steady state, but it varies according to the load-varying conditions in transient periods according to Eq. (13),

$$\begin{bmatrix} V_{\alpha S}^{MG,i} \\ V_{\beta S}^{MG,i} \end{bmatrix} = \begin{bmatrix} 1 & -1/2 & 1/2 \\ 0 & \sqrt{3}/2 & -\sqrt{3}/2 \end{bmatrix} \begin{bmatrix} V_{aS}^{MG,i} \\ V_{bS}^{MG,i} \\ V_{cS}^{MG,i} \end{bmatrix} \tag{13}$$

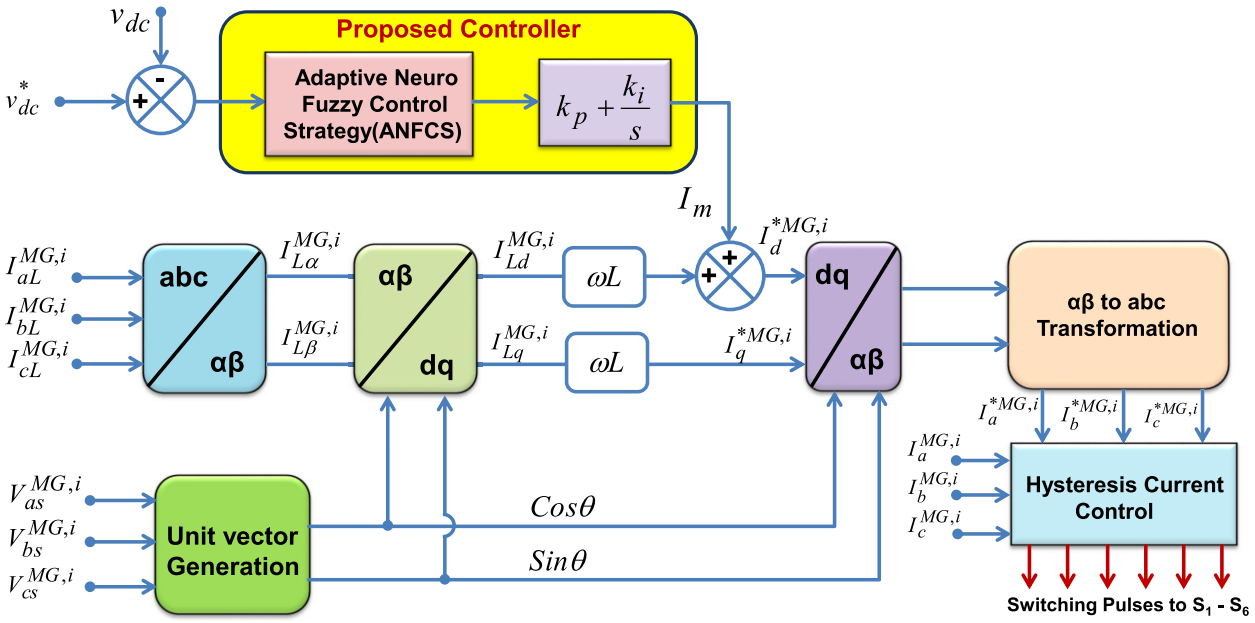

FIGURE 10. Inverter control strategy for i[th] microgrid using the proposed controller.

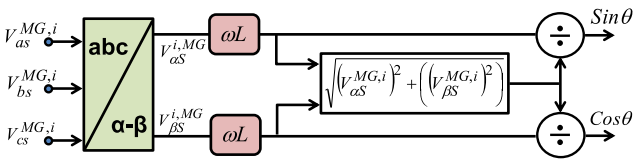

FIGURE 11. Block diagram representation of unit vector model for an i[th] microgrid.

By simplifying Eq. (13), we get the voltage coordinates as given in Eq. (14) and Eq. (15).

$$V_{\alpha S}^{MG,i} = \frac{\sqrt{3}}{2} V_P.Sin(\omega t) \tag{14}$$

$$V_{\beta S}^{MG,i} = \frac{\sqrt{3}}{2} V_P.Cos(\omega t) \tag{15}$$

where, $V_{aS}^{MG,i}$, $V_{bS}^{MG,i}$, $V_{cS}^{MG,i}$ are sources voltages, $V_{\alpha S}^{MG,i}$ and $V_{\beta S}^{MG,i}$ are stationary frame variables of an i[th] microgrid, V_P is the peak value of the source voltage, and 'ω' is the fundamental angular frequency of an i[th] microgrid.

An easy-to-use method is used to calculate the unit vector model's output to create the synchronization vector in the proposed scheme, as shown in Fig. 11.

According to the definition of the unit vector, $Cos\theta$ and $Sin\theta$ can be obtained using Eq. (16) and Eq. (17).

$$\left.\begin{aligned} Cos\theta &= \frac{V_{\alpha S}^{MG,i}}{\sqrt{\left(V_{\alpha S}^{MG,i}\right)^2 + \left(V_{\beta S}^{MG,i}\right)^2}} = \frac{\frac{\sqrt{3}}{2} V_P Sin\omega t}{\frac{\sqrt{3}}{2} V_P} \\ &= Sin\omega t \end{aligned}\right\} \tag{16}$$

$$\left.\begin{aligned} Sin\theta &= \frac{V_{\alpha S}^{MG,i}}{\sqrt{\left(V_{\alpha S}^{MG,i}\right)^2 + \left(V_{\beta S}^{MG,i}\right)^2}} = \frac{-\frac{\sqrt{3}}{2} V_P Sin\omega t}{\frac{\sqrt{3}}{2} V_P} \\ &= -Cos\omega t \end{aligned}\right\} \tag{17}$$

This approach has the benefit of being frequency independent because angle 'θ' is calculated directly from the source voltage. The algorithm is further extended to compute the desired reference current signals once the necessary harmonics components have been removed from the distorted load current; as a result, the d-q rotating frame is converted back to the α-β stationary frame as given in Eq. (18). And, the reference currents are expressed from α-β stationary frame given in Eq. (19).

$$\begin{bmatrix} I_\alpha^{*MG,i} \\ I_\beta^{*MG,i} \end{bmatrix} = \begin{bmatrix} Sin\theta & -Cos\theta \\ Cos\theta & Sin\theta \end{bmatrix}^{-1} \begin{bmatrix} I_d^{*MG,i} \\ I_q^{*MG,i} \end{bmatrix} \tag{18}$$

$$\begin{bmatrix} I_\alpha^{*MG,i} \\ I_\beta^{*MG,i} \end{bmatrix} = \begin{bmatrix} Sin\theta & Cos\theta \\ -Cos\theta & Sin\theta \end{bmatrix} \begin{bmatrix} I_d^{*MG,i} \\ I_q^{*MG,i} \end{bmatrix} \tag{19}$$

From Fig. 10, it is d-axis reference current can be obtained as given in Eq. (20),

$$I_d^{*MG,i} = I_m + I_{Ld}^{MG,i} \tag{20}$$

where the loss component value at m^{th} sampling instant I_m for meeting the losses in i[th] MG is obtained as given in Eq. (21).

$$I_m^{MG,i} = I_{m-1}^{MG,i} + K_{pd}\left(\left(V_{dc}^* - V_{dc}\right)_m - \left(V_{dc}^* - V_{dc}\right)_{(m-1)}\right) + K_{id}\left(V_{dc}^* - V_{dc}\right)_m \tag{21}$$

where K_{pd} and K_{id} are PI controller gains that are tuned by the proposed control strategy. Now, convert the above stationary

frame reference currents into three-phase reference currents using Eq. (22) as follows.

$$\begin{bmatrix} I_a^{*MG,i} \\ I_b^{*MG,i} \\ I_c^{MG,i} \end{bmatrix} = \sqrt{\frac{2}{3}} \begin{bmatrix} 1 & 0 \\ -1/2 & \sqrt{3}/2 \\ 1/2 & -\sqrt{3}/2 \end{bmatrix} \begin{bmatrix} I_\alpha^{*MG,i} \\ I_\beta^{*MG,i} \end{bmatrix} \quad (22)$$

The above reference currents obtained in Eq. (22) are applied to the hysteresis controller. Later these currents are compared with the source currents, and the switching pulses will be produced at their output terminals.

IV. RESULTS AND DISCUSSION

To determine the efficacy of the proposed ANFCS control technique for the inverter of ith microgrid and DSTATCOM, various power quality parameters such as voltage swell/sag, voltage imbalance, frequency deviations, and total harmonic distortion are considered under different test conditions. Modeling the proposed MMGs cluster and the control technique are done using MATLAB/Simulink 2021, a program with a runtime version of 9.1 for Windows 64-bit.

A. VOLTAGE CHARACTERISTICS

Voltage sag is a short-duration drop in voltage magnitude. These are mainly due to the fast application of load currents or faults. Similarly, sudden removal of the load causes to decrease in source current during voltage swells and increases the voltage magnitude. In this section, the performance of the proposed MMGs cluster system with a control technique with P.I., Fuzzy, and proposed ANFCS controllers for the inverter of an ith microgrid is verified by applying different test conditions for the measurement of voltage sag/swell at the PCC of the cluster. The cluster's PCC voltage is maintained at 415v, 50Hz.

To measure the voltage sag and swell, initially, the proposed system is associated with a base load of 250kW. A test load of 650kW is injected into the system from 0.1sec to 0.2sec to observe the sag of the system with all the controllers. It is observed from the sag zone results, as shown in Fig. 12(a) to Fig. 12(c), that sag is 42.5% with P.I., 40.05% with Fuzzy, and 12.5% with proposed ANFCS controllers. A portion of the base load (70%, i.e., 175kW) from 0.3sec to 0.4sec is to be disconnected from the system that is already linked to observe the voltage swell. The swell zone shown in Fig. 12(a) to 12(c) shows the voltage sag swell is 2.43% with PI, 3.7% with Fuzzy, and 2.9% with proposed ANFCS controllers.

Microgrids have many single-phase sources and loads leading to imbalanced voltage. Voltage imbalance lowers the quality of the power, which causes client equipment and the microgrid to malfunction or fail. Additionally, induction motors, power electronic converters, and variable speed drives are also severely impacted by voltage unbalance. The voltage imbalances in a system are computed by Eq. (23).

$$\%imbalance = \frac{V_{M.D}\,(PU)}{V\,(PU)}\bigg|_{average} \quad (23)$$

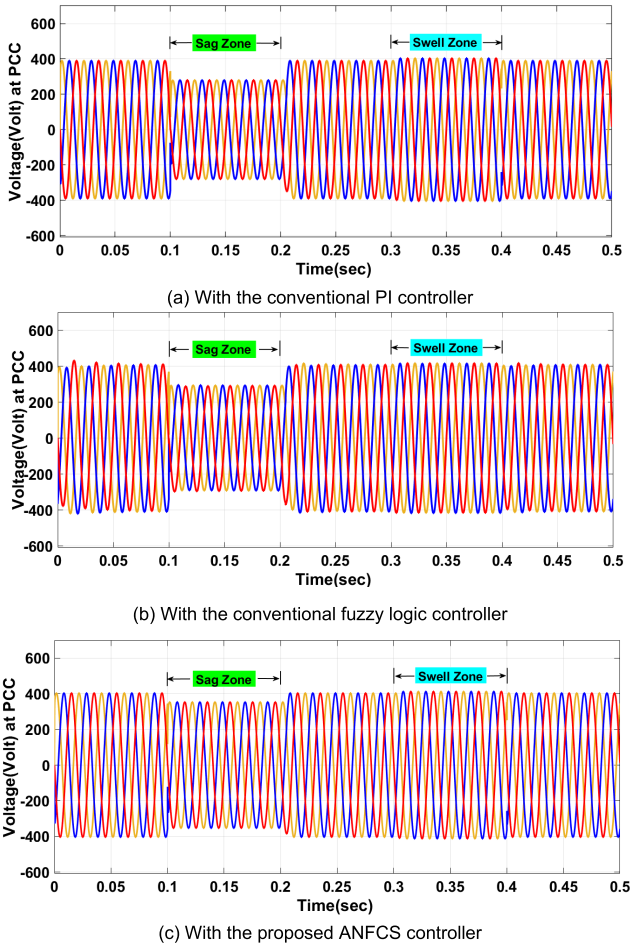

FIGURE 12. Voltage sag/swell at the PCC of the multi-microgrid cluster.

where $V_{M.D}$ is the maximum deviation in voltage from its average value in PU and V is the average voltage of the system.

Inject a load of j30kVAR (inductive load), coupled with a base load of 375kW+j85kVAR and a test load of j75kVAR, in phase "a" at 0.1sec to analyze the voltage imbalances through positive and negative sequence components. Figure 13 depicts the simulation results, and it can be seen that the voltage imbalance is 9.36% with PI, 4.78% with Fuzzy, and 2.94% with proposed ANFCS controllers. The results also indicate that some transients may occur during sudden load injection in the system. According to the quantitative results obtained from simulations, the proposed ANFCS controller produces better results than the conventional ANFCS controller. For accuracy, the results are compared per IEEE/IEC standards and tabulated [26], [27], [28], [29].

B. NEUTRAL CURRENT COMPENSATION

Overloading of a distribution feeder and transformer is caused by an excessive neutral current level due to unbalance and also results in heat losses. Additionally, the performance

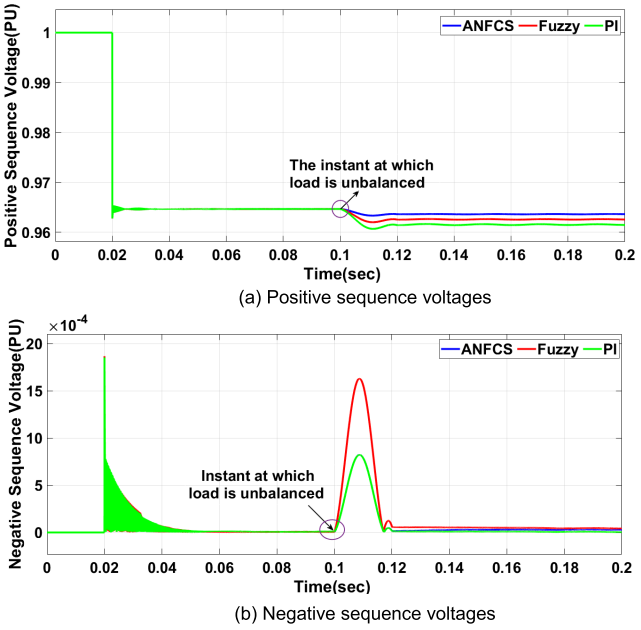

FIGURE 13. Voltage imbalances at PCC of the multi-microgrid cluster.

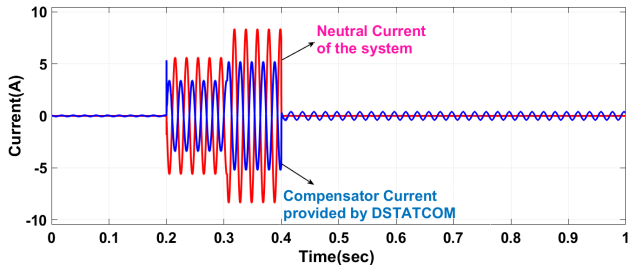

FIGURE 14. Neutral current compensation at PCC of the cluster.

of delicate electronic devices connected to the network is impacted by common mode voltage induced by the neutral current. The assessment of neutral current imbalances of the system is given in Eq. (24) [23].

$$I_{N,PCC} = \sqrt{\left(I_a^2 + I_b^2 + I_c^2 - I_a I_b - I_b I_c - I_c I_a\right)\big|_{PCC}} \quad (24)$$

where, I_a, I_b, I_c are the RMS values of phase currents; In Fig. 14, the neutral current supplied by the DSTATCOM with the proposed control strategy is shown. So the proposed controller strategy effectively reduces the neutral current at the PCC of the cluster.

C. POWER CHARACTERISTICS

To observe the transient variations in real and reactive power characteristics of the proposed multi-microgrid cluster system, huge reactive loads are injected at the PCC. A base load of 375kW+j85kVAR and a test load of j175kVAR inductive load are injected from 0.1sec to 0.2sec, and -j100kVAR capacitive load is injected from 0.3sec to 0.4sec.

The simulation results given in Fig. 15(a) and Fig. 15(b) show how the active and reactive powers vary for the injected

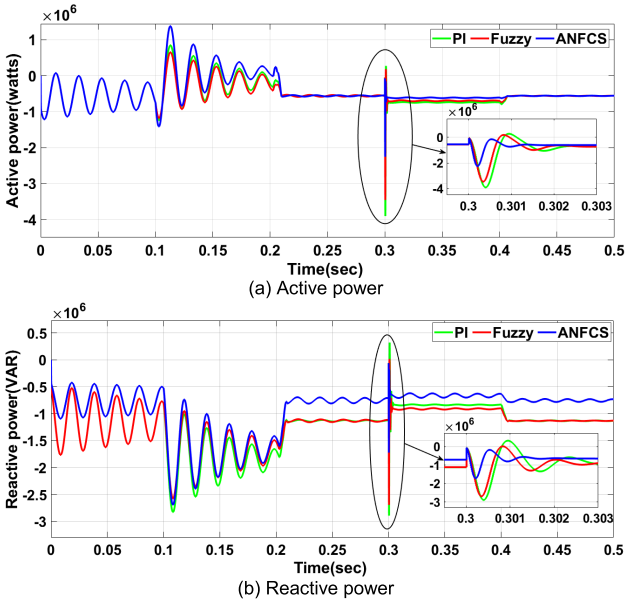

FIGURE 15. Active and reactive power responses at PCC of the cluster.

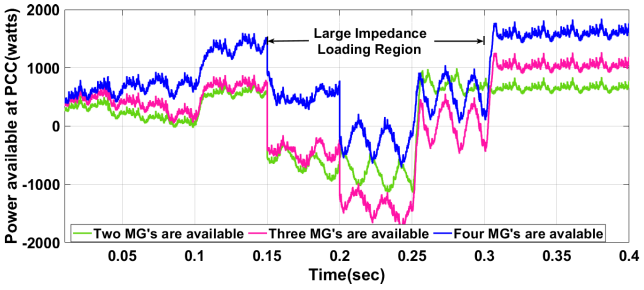

FIGURE 16. Power availability at PCC of the cluster in different cases.

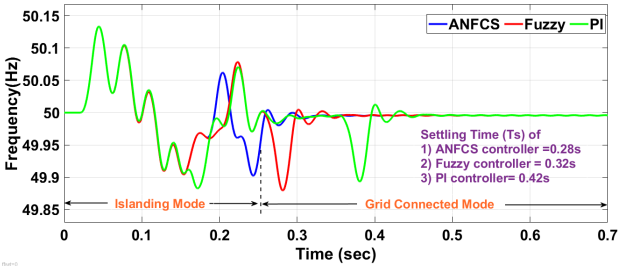

FIGURE 17. Frequency response at the PCC of the cluster with conventional PI, Fuzzy, and proposed ANFCS controllers.

loads at the PCC of the cluster. These results show the reduced transient deviation in the characteristics obtained with the proposed controller when compared with the remaining two conventional controllers, thereby justifying the importance of the proposed controller to the inverters of the multi-microgrid cluster application.

Figure 16 depicts the power availability at PCC of the cluster when only two of the MGs are available, three of the MGs are available, and all four MGs are available at a given point of time respectively. In the system, all the

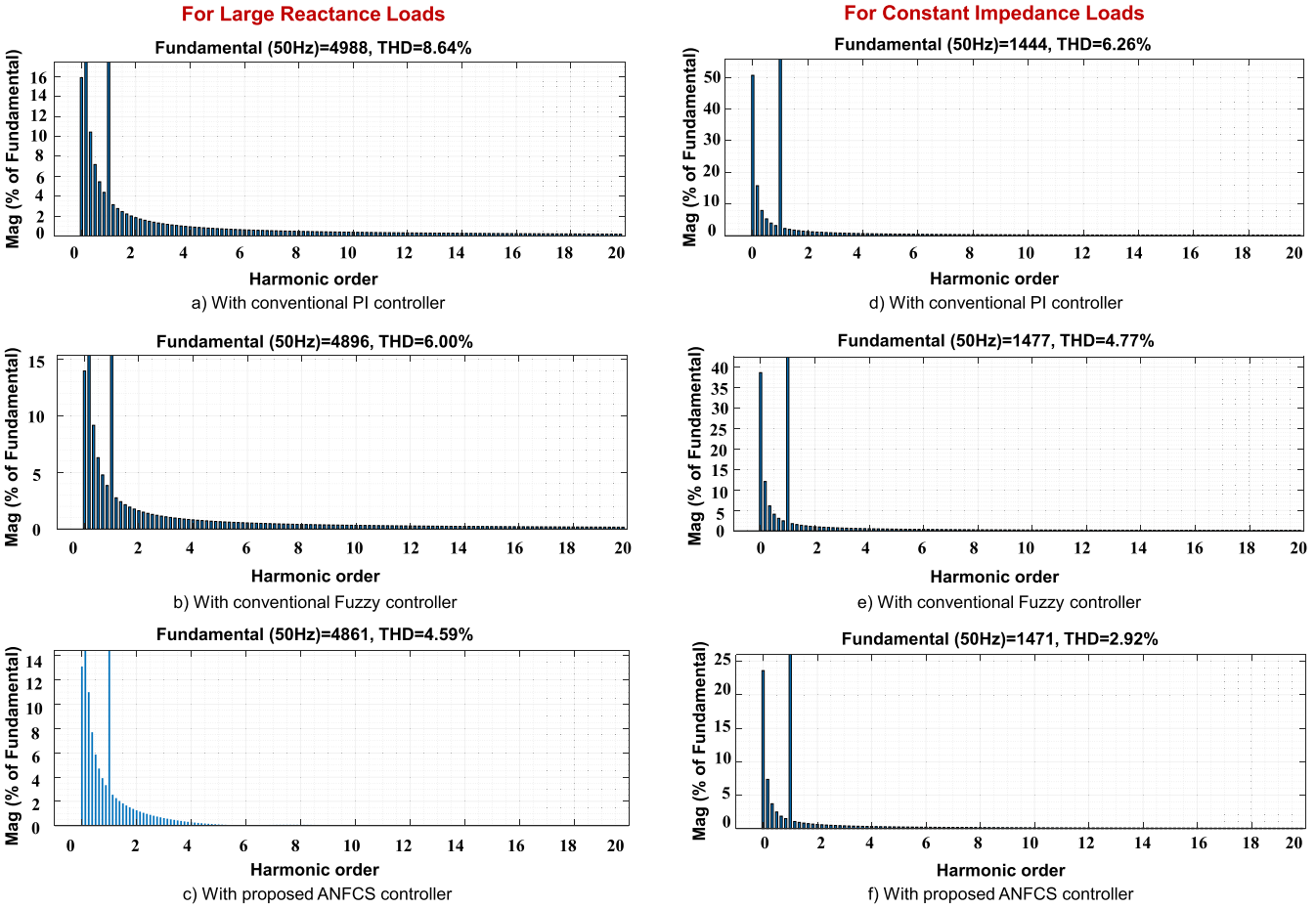

FIGURE 18. Total harmonic distortion of the multi-microgrid cluster with conventional PI, Fuzzy, and proposed ANFCS controllers.

load variations are applied from 0.1sec to 0.3sec, in which, a large impedance load is applied between 0.15sec to 0.3sec to observe the power availability at the PCC of the cluster. In all cases, a combination of four microgrids shows superiority when compared with a combination of two microgrids and three microgrids. This shows the importance of integrating multiple microgrids as a cluster. However, imports from the utility grid are made available when there is a shortage in the cluster due to the unavailability of any cluster microgrids.

D. FREQUENCY RESPONSE CHARACTERISTICS

Frequency is a crucial characteristic that needs to be continuously monitored and regulated when the cluster microgrids are run in grid-connected/autonomous mode. To analyze the frequency response, an impedance load of 475kW+j250kVAR-j150kVAR is injected at the PCC of the microgrid cluster from 0sec to 0.7sec to identify the effectiveness of various controllers used. From Fig. 17, it is observed that whenever the system operates under the islanded mode, some fluctuations exist in the response from 0sec to 0.2sec. As per IEEE std. the deviation in frequency must be 1% [30], [31].

E. TOTAL HARMONIC DISTORTION

Harmonics are non-sinusoidal voltage or current waveforms with frequencies different from the fundamental frequency. In general, nonlinear current and voltage characteristics of equipment already present in the power system can lead to harmonic distortion. Current harmonics dominance in the power network is mainly caused by nonlinear loads and power electronics converters.

The injected current harmonics might also increase the voltage harmonics in the power network due to the system impedance. The following problems might result from excessive harmonics in a power network: voltage distortion on the secondary side of the distribution, overloading of the neutral in a three-phase power system, and overheating transformers and cables. Transformers in power system networks increase system power loss, impact measuring instrument performance, which causes protective relays to malfunction, increase dielectric losses and thermal stress in capacitor banks, and increase copper loss and heat loss in electrical equipment, among other things. The following loads are introduced into the system to study the impact of a significant impedance load on it. From 0.04sec to 0.1sec, 150 kW+75kVAR load is applied, between 0.08sec

TABLE 2. Quantitative comparison of PQ parameters obtained with various controllers.

Power Quality Indices		Controller Used to Control the Multi-microgrid Based Cluster			Standard Requirements
		Conventional PI [10]	Conventional Fuzzy [20]	Proposed ANFCS	
Voltage characteristics	Sag	42.5 % (violated)	40.5 % (violated)	12.5 %	40% [26, 27]
	Swell	2.43 %	3.7 %	2.9 %	
	Unbalance	9.36 % (violated)	4.78 % (violated)	2.94 %	3% [28, 29]
Frequency characteristics	Settling time	0.42 sec	0.32 sec	0.28 sec	Deviation of 1% [30, 31]
Total harmonic distortion (THD)	With large reactance loads	8.64 % (violated)	6.00 % (violated)	4.59 %	5% [32, 33]
	With large impedance loads	6.26 % (violated)	4.77 %	2.92 %	

to 0.16 sec, 345 kW+80kVAR load is applied, and between 0.12sec and 0.2sec, 750 kW load is injected into the system. Similarly, the loads are introduced into the system to study the impact of a significant reactive load on it. Switch on the 175kVAR load that is already connected at 0.12sec. The 275kW base load must also be switched off at 0.12sec. Figure 18 displays all the simulation findings with various controllers used in the proposed system for testing THD characteristics.

The fruitfulness of the proposed controller can be observed from the quantitative results given in Table 2. In this table, the proposed methodology is compared with the techniques used in the literature and with IEEE/IEC standards [32], [33]. Considering all the results obtained through simulation analysis, it is concluded that the proposed controller (ANFCS) performs well when compared with the remaining two controllers (conventional PI and Fuzzy).

V. CONCLUSION

This paper proposed the concept of ANFCS controller to multi-microgrids based cluster to improve its power quality. Various indices such as voltage sag/swell, frequency response, total harmonic distortion, neutral current compensation, and power characteristics are analyzed and measured quantitatively for the proposed system. From these cumulative results, the salient merits of the proposed controller are summarized as follows.

- The voltage sag measured from the results is 42.5% with the conventional PI controller and 40.5% with the conventional Fuzzy controller, which are violating according to IEC 61000-4-11. But, the sag deviation is significantly less with the proposed controller, which is observed as 12.5%. Similarly, there is a slight improvement in voltage swell with all the controllers viz., 2.43% with PI, 3.7% with Fuzzy, and 2.9% with proposed ANFCS.
- The voltage imbalances are also violated with the use of conventional PI (9.36%) and conventional Fuzzy (4.78%) controllers. While the proposed controller limits the voltage imbalances to a tolerable value (2.94%) that is defined by IEEE 1159.3.
- The settling time of the proposed system with various controllers is analyzed. From the quantitative results, it is to be noted that the frequency response of the cluster microgrid takes significantly less time to settle in the steady state with the proposed ANFCS controller (0.28 sec) when compared with conventional PI (0.42 sec) and conventional Fuzzy (0.32 sec). Due to the less settling time, the steady-state stability is improved with the proposed controller.
- From the results of the THD, it is concluded that, in the case of large reactive and impedance loading conditions, the proposed controllers performed well when compared with the remaining controllers.

Thus, based on the results obtained in this study, it is concluded that the proposed ANFCS controller has fruitfully outperformed the conventional PI and Fuzzy based controllers, thereby enhancing the usefulness of the microgrid deployments.

DATA AVAILABILITY STATEMENT

Not applicable.

CONFLICTS OF INTEREST

The authors declare no conflict of interest.

REFERENCES

[1] S. N. V. B. Rao, Y. V. P. Kumar, D. J. Pradeep, C. P. Reddy, A. Flah, H. Kraiem, and J. F. Al-Asad, "Power quality improvement in renewable-energy-based microgrid clusters using fuzzy space vector PWM controlled inverter," *Sustainability*, vol. 14, no. 8, p. 4663, Apr. 2022, doi: 10.3390/su14084663.

[2] Y. V. P. Kumar and B. Ravikumar, "Integrating renewable energy sources to an urban building in India: Challenges, opportunities, and techno-economic feasibility simulation," *Technol. Econ. Smart Grids Sustain. Energy*, vol. 1, no. 1, pp. 1–16, Dec. 2016, doi: 10.1007/s40866-015-0001-y.

[3] Y. V. P. Kumar and R. Bhimasingu, "Electrical machines based DC/AC energy conversion schemes for the improvement of power quality and resiliency in renewable energy microgrids," *Int. J. Electr. Power Energy Syst.*, vol. 90, pp. 10–26, Sep. 2017, doi: 10.1016/j.ijepes.2017.01.015.

[4] S. N. V. B. Rao and K. Padma, "A review on schemes for interconnecting microgrids of urban buildings," in *Microelectronics, Electromagnetics and Telecommunications* (Lecture Notes in Electrical Engineering), vol. 655. Singapore: Springer, 2021, doi: 10.1007/978-981-15-3828-5_45.

[5] I. Mahendravarman, S. A. Elankurisil, M. Venkateshkumar, A. Ragavendiran, and N. Chin, "Artificial intelligent controller-based power quality improvement for microgrid integration of photovoltaic system using new cascade multilevel inverter," *Soft Comput.*, vol. 24, no. 24, pp. 18909–18926, Dec. 2020, doi: 10.1007/s00500-020-05120-2.
[6] T. E. Rao, K. M. Tatikonda, S. Elango, and J. C. Kumar, "Power quality improvement in microgrid system using PSO-based UPQC controller," in *Microgrid Technologies*. Beverly, MA, USA: Scrivener Publishing LLC, 2021, ch. 11, pp. 287–307, doi: 10.1002/9781119710905.ch11.
[7] A. H. Elmetwaly, A. A. Eldesouky, and A. A. Sallam, "An adaptive D-FACTS for power quality enhancement in an isolated microgrid," *IEEE Access*, vol. 8, pp. 57923–57942, 2020, doi: 10.1109/ACCESS.2020.2981444.
[8] J. Liu, S. Taghizadeh, J. Lu, M. J. Hossain, S. Stegen, and H. Li, "Three-phase four-wire interlinking converter with enhanced power quality improvement in microgrid systems," *CSEE J. Power Energy Syst.*, vol. 7, no. 5, pp. 1064–1077, 2021, doi: 10.17775/CSEEJPES.2020.01850.
[9] M. Amir, A. K. Prajapati, and S. S. Refaat, "Dynamic performance evaluation of grid-connected hybrid renewable energy-based power generation for stability and power quality enhancement in smart grid," *Front. Energy Res.*, vol. 10, Mar. 2022, Art. no. 861282, doi: 10.3389/fenrg.2022.861282.
[10] A. Kumar, R. Garg, and P. Mahajan, "Modified synchronous reference frame control of solar photovoltaic-based microgrid for power quality improvement," *Arabian J. Sci. Eng.*, vol. 46, no. 2, pp. 1001–1018, Feb. 2021, doi: 10.1007/s13369-020-04789-9.
[11] S. Musa, M. Radzi, H. Hizam, N. Wahab, Y. Hoon, and M. Zainuri, "Modified synchronous reference frame based shunt active power filter with fuzzy logic control pulse width modulation inverter," *Energies*, vol. 10, no. 6, p. 758, May 2017, doi: 10.3390/en10060758.
[12] S. R. Das, P. K. Ray, A. K. Sahoo, K. K. Singh, G. Dhiman, and A. Singh, "Artificial intelligence based grid connected inverters for power quality improvement in smart grid applications," *Comput. Electr. Eng.*, vol. 93, Jul. 2021, Art. no. 107208, doi: 10.1016/j.compeleceng.2021.107208.
[13] A. Ab-BelKhair, J. Rahebi, and A. A. M. Nureddin, "A study of deep neural network controller-based power quality improvement of hybrid PV/wind systems by using smart inverter," *Int. J. Photoenergy*, vol. 2020, pp. 1–22, Dec. 2020, doi: 10.1155/2020/8891469.
[14] J. Alshehri and M. Khalid, "Power quality improvement in microgrids under critical disturbances using an intelligent decoupled control strategy based on battery energy storage system," *IEEE Access*, vol. 7, pp. 147314–147326, 2019, doi: 10.1109/ACCESS.2019.2946265.
[15] D. R. Nair, M. G. Nair, and T. Thakur, "A smart microgrid system with artificial intelligence for power-sharing and power quality improvement," *Energies*, vol. 15, no. 15, p. 5409, Jul. 2022, doi: 10.3390/en15155409.
[16] M. F. Ullah and A. Hanif, "Power quality improvement in distribution system using distribution static compensator with super twisting sliding mode control," *Int. Trans. Electr. Energy Syst.*, vol. 31, no. 9, Sep. 2021, Art. no. e12997, doi: 10.1002/2050-7038.12997.
[17] S. R. Das, P. K. Ray, A. K. Sahoo, K. Balasubramanian, and G. S. Reddy, "Improvement of power quality in a three-phase system using an adaline-based multilevel inverter," *Frontiers Energy Res.*, vol. 8, p. 23, Feb. 2020, doi: 10.3389/fenrg.2020.00023.
[18] D. P. Acharya, N. Nayak, S. Choudhury, and R. Padhy, "Power quality improvement in a fuel-cell based micro-grid with shunt active power filter," *Int. J. Renew. Energy Res.*, vol. 10, no. 3, pp. 1071–1082, 2020, doi: https://doi.org/10.20508/ijrer.v10i3.10698.g7981.
[19] S. N. V. B. Rao, V. P. K. Yellapragada, K. Padma, D. J. Pradeep, C. P. Reddy, M. Amir, and S. S. Refaat, "Day-ahead load demand forecasting in urban community cluster microgrids using machine learning methods," *Energies*, vol. 15, no. 17, p. 6124, Aug. 2022, doi: 10.3390/en15176124.
[20] Y. V. P. Kumar, S. N. V. Rao, K. Padma, C. P. Reddy, D. J. Pradeep, A. Flah, H. Kraiem, M. Jasinski, and S. Nikolovski, "Fuzzy hysteresis current controller for power quality enhancement in renewable energy integrated clusters," *Sustainability*, vol. 14, no. 8, p. 4851, Apr. 2022, doi: 10.3390/su14084851.
[21] M. Mao, P. Jin, N. D. Hatziargyriou, and L. Chang, "Multiagent-based hybrid energy management system for microgrids," *IEEE Trans. Sustain. Energy*, vol. 5, no. 3, pp. 938–946, Jul. 2014, doi: https://doi.org/10.1109/TSTE.2014.2313882.
[22] Y. Zheng, Y. Song, D. J. Hill, and Y. Zhang, "Multiagent system based microgrid energy management via asynchronous consensus ADMM," *IEEE Trans. Energy Convers.*, vol. 33, no. 2, pp. 886–888, Jun. 2018, doi: https://doi.org/10.1109/TEC.2018.2799482.
[23] A. Vinayagam, K. Swarna, S. Y. Khoo, and A. Stojcevski, "Power quality analysis in microgrid: An experimental approach," *J. Power Energy Eng.*, vol. 4, no. 4, pp. 17–34, 2016, doi: 10.4236/jpee.2016.44003.
[24] A. Ramadan, S. Kamel, I. Hamdan, and A. M. Agwa, "A novel intelligent ANFIS for the dynamic model of photovoltaic systems," *Mathematics*, vol. 10, no. 8, p. 1286, Apr. 2022, doi: 10.3390/math10081286.
[25] M. A. Islam, J. G. Singh, I. Jahan, M. S. H. Lipu, T. Jamal, R. M. Elavarasan, and L. Mihet-Popa, "Modeling and performance evaluation of ANFIS controller-based bidirectional power management scheme in plug-in electric vehicles integrated with electric grid," *IEEE Access*, vol. 9, pp. 166762–166780, 2021, doi: 10.1109/ACCESS.2021.3135190.
[26] *IEEE Recommended Practice for Electric Power Distribution for Industrial Plants*, IEEE Standard 141–1993, (Revision of ANSI/IEEE Standard 141-1986), pp. 1–768, 1994.
[27] *Electromagnetic Compatibility (EMC)—Part 4-34: Electromagnetic Compatibility (EMC)—Part 4-11: Testing and Measurement Techniques—Voltage Dips, Short Interruptions and Voltage Variations Immunity Tests for Equipment With Input Current Up to 16 A Per Phase*, Standard IEC 61000-4-11:2020, 2020.
[28] *IEEE Recommended Practice for Power Quality Data Interchange Format (PQDIF)*, IEEE Standard 1159.3-2019, (Revision of IEEE Std. 1159.3-2003), pp. 1–185, May 2019, doi: 10.1109/IEEESTD.2019.8697192.
[29] K. Antoni and B. P. Marta. *Voltage Characteristics of Electricity Supplied by Public Electricity Networks*, Standard EN 50160, 2019. [Online]. Available: http://www.leonardo-energy.org
[30] *Photovoltaic (P.V.) Systems—Characteristics of the Utility Interface*, Standard IEC 61727:2004, 2004. [Online]. Available: https://webstore.iec.ch/publication/5736
[31] *Electromagnetic compatibility (EMC)—Part 2-2: Environment-Compatibility Levels for Low-Frequency Conducted Disturbances and Signaling in Public Low-Voltage Power Supply Systems*, Standard IEC 61000-2-2, 2002. [Online]. Available: https://webstore.iec.ch/publication/4133
[32] *IEEE Standard Conformance Test Procedures for Equipment Interconnecting Distributed Energy Resources With Electric Power Systems and Associated Interfaces*, IEEE Standard 1547.1-2020, pp. 1–282, 2020, doi: 10.1109/IEEESTD.2020.9097534.
[33] *IEEE Recommended Practice and Requirements for Harmonic Control in Electric Power Systems*, IEEE Standard 519–2014, (Revision of IEEE Std. 519-1992), pp. 1–29, 2014, doi: 10.1109/IEEESTD.2014.6826459.

S. N. V. BRAMARESWARA RAO was born in Eluru, Andhra Pradesh, India, in 1987. He received the B.E. degree in electrical and electronics engineering, the M.E. degree in power systems and automation and the Ph.D. degree from Andhra University, Visakhapatnam, in 2008, 2015, and 2022, respectively.

He has 13 years of teaching experience, including five years of research experience. Currently, he is working as an Associate Professor with the Department of EEE, Sir C. R. Reddy College of Engineering, Eluru. He published several research papers in national/international conferences/journals. He is an Active Reviewer of IEEE, Tailor and Francis, Wiley, *IJCDS*, and *Bulletin of Electrical Engineering and Informatics*. His research interests include hybrid power systems, microgrids, renewable energy sources, AI applications to power systems, and power quality.

Y. V. PAVAN KUMAR (Member, IEEE) was born in Tenali, Andhra Pradesh, India, in 1985. He received the B.Tech. degree in electrical and electronics engineering from the JNT University, Hyderabad, Telangana, India, in 2007, the M.Tech. degree in instrumentation and control systems from the University College of Engineering, JNTUK University, Kakinada, Andhra Pradesh, in 2011, and the Ph.D. degree in electrical engineering from the IITH, Telangana, in 2018.

From 2007 to 2009, he was an Assistant Professor at the Sir C. R. Reddy College of Engineering, Eluru, Andhra Pradesh, India, and from 2011 to 2014, he was a System Engineer at Honeywell Technology Solutions (Pvt.) Ltd., Hyderabad. Since 2017, he has been an Associate Professor with the School of Electronics Engineering, VIT-AP University, Amaravati, Andhra Pradesh. He is the author of three books, 125 papers, and 24 patents. His research interests include microgrids, smart grids (data analytics and communications), electric vehicles, power quality, advanced control, and power converters.

Dr. Kumar was a recipient of the SERB SIRE Fellowship, in 2022, the SERB SRG Grant, from 2019 to 2022, the IEEE-IES STPA Award 2016, the IIT Hyderabad Research Excellence Award, in 2014, 2015, and 2016, the Honeywell International-ETS Global Excellence Award, Canada, in 2012, the Partner Excellence Award from EMS Aviation, Moorestown, USA, in 2012, the Best Paper/ Presentation Award at various international conferences namely Springer VICFCNT-2021 India, Springer RAAI-2020, India, IEEE IECON-2016, Italy, and IET SEISCON-2011, India. He was recognized as a Standard Reviewer from ELSEVIER. He was a Nominated Member of the Electronics and Information Technology Department (LITD 27 'Internet of Things and related technologies sectional committee), Bureau of Indian Standards (BIS), India, and a member of ISO/IEC JTC 1/SC 41 Internet of Things and Digital Twin. He is an Associate Editor of the *International Journal of Advances in Applied Sciences* (IJAAS), the *International Journal of Electrical and Computer Engineering* (IJECE), and *TELKOMNIKA (Telecommunication, Computing, Electronics and Control)*.

MOHAMMAD AMIR (Member, IEEE) received the B.Tech. degree in electrical engineering from Integral University, Lucknow, India, in 2015, and the M.Tech. degree in specialization of power electronics and drives from the Madan Mohan Malaviya University of Technology (MMMUT), Gorakhpur, India, in 2018.

He is working as a Researcher with the Advanced Power Electronics Research Laboratory, Department of Electrical Engineering, Faculty of Engineering and Technology, Jamia Millia Islamia (A Central University), New Delhi, India. He has research experience in Department of Heavy Industry (DHI), Government of India (under India Fame Mission). He has published many patents, journals, book chapters, and international conferences. His current research interests include intelligent optimization techniques, renewable energy, smart energy management, electric vehicle, energy storage, and smart grid. He is currently an Associate Member of International Society of Energy and Built Environment, Australia, and International Society for Energy Transition Studies. He is a member of Autonomous Vehicles and Systems, ASME, USA. He was a recipient of the Ministry of Human Resource Development (MHRD) Fellowship. He was a fellow of Graduate Aptitude Test in Engineering (GATE) in specialization of electrical engineering, from 2016 to 2019, and Qualified of Faculty Aptitude Test of Engineering (FATE) conducted by AKTU, in 2018. He is actively IEEE Young Professional of Asia Pacific. He has done various research in government funded programs. He is Research and Academic Coordinator, IEEE Delhi Section, India, Region-10, in 2021 and 2022. He is a reviewer of many prestigious journals and conferences. He is an Editor of *Frontiers in Energy Research* and *Frontiers in Future Transportation*.

FURKAN AHMAD (Member, IEEE) received the B.Tech., M.Tech., and Ph.D. degrees in electrical engineering from Aligarh Muslim University, India, in 2012, 2015, and 2019, respectively. He is working as a Researcher with Hamad Bin Khalifa University, Qatar Foundation, Doha, Qatar. He was awarded the CSIR Junior and Senior Research Fellowship Award, from 2016 to 2019. He joined IIT Delhi as a Postdoctoral Fellow. He has authored/coauthored more than 60 research articles. His research interests include microgrids, electric vehicles, charging infrastructure, grid integration, and energy management systems. He is also an Associate Editor of *Frontiers in Energy Research*, *International Journal on Smart Sensing and Intelligent Systems*, and *Frontiers in Future Transportation*.